Experimental investigation on evaporative cooling coupled phase change energy storage technology for data centers under natural air cooling

Xiaoyan Yi [a], Hongli Xu [a], Ruiyong Mao [a], Hongwei Wu [b], Xiangkui Gao [c], Jiri Zhou [d], Zujing Zhang [a*]

[a] College of Civil Engineering, Guizhou Provincial Key Laboratory of Rock and Soil Mechanics and Engineering Safety, State Key Laboratory of Public Big Data, Guizhou University, Guiyang, 550025, China.

[b] School of Physic, Engineering and Computer Science, University of Hertfordshire, Hatfield, AL10 9AB, United Kingdom.

[c] State Key Laboratory for Geo Mechanics and Deep Underground Engineering, China University of Mining and Technology, Xuzhou, Jiangsu, 221116, China

[d] China MCC5 Group CORP.LTD.

[*]Corresponding author: tel: coupled86 185 2391 9513. email: zjzhang3@gzu.edu.cn.

Abstract: To address the challenges of prolonged cooling air supply for data centers (DCs) in high-temperature climates, a cooling ventilation system combining evaporative cooling with phase change energy storage (PCES) under natural air cooling is proposed. Based on the summer high-temperature meteorological conditions in Gui'an New District, Guizhou Province, China, experiments were conducted using single-factor impact analysis and orthogonal experiments. These experiments investigated the effects of several control parameters such as inlet air temperature, inlet speed, inlet humidity, and spray flow on the cooling performance of the integrated cooling device, confirming the feasibility and high efficiency of this technology for green DCs. The results indicate that: (1) After being treated for temperature and humidity through the spray and the phase change plate (PCP) at both ends, the air temperature can be lowered by about 7 °C on average, and the relative humidity can be reduced by about 35% over an 8-hour period. (2) The temperature difference between inlet and outlet increases with the increase of inlet air temperature and spray flow but decreases with the increase of inlet air speed and inlet air humidity. (3) Through orthogonal experiments, the major and minor factors affecting the cooling performance, in order of significance, are inlet air temperature > inlet speed > spray flow > inlet humidity.

Keywords: Natural cooling; Evaporative cooling; Phase change energy storage; Data centers; Orthogonal experiments

Nomenclature

Greek symbols		Abbreviation	
S_σ^2	Sample variance	DC	Data center
x_i	Measurement value obtained from the ith measurement, i=1, 2, 3 ...... n	PCP	Phase change plates
$\bar{x}$	Arithmetic mean of n measurements	PCM	Phase change materials
n	Number of measurements	PCES	Phase change energy storage
$\hat{\sigma}$	Standard deviation	DEC	Direct evaporative cooling

1. Introduction

With the rapid evolution of cloud computing and big data, data centers (DCs) have become crucial infrastructure for information processing and storage in modern society [1]. As of the end of 2021, there were over 700 hyperspace DCs in operation worldwide [2]. However, the high energy consumption and heat dissipation of DCs have emerged as significant constraints to their sustainable expansion [3]. It is estimated that by 2030, DCs could consume up to 51 % of the world's electricity demand [4]. Servers and cooling systems are the primary energy-consuming devices within DCs [5], with refrigeration system alone accounting for approximately 40% of total energy consumption [6]. Therefore, a critical focus in ensuring the sustainability of DCs is reducing the energy consumption of their cooling systems.

Free cooling technology, also known as economizer circulation, is an energy-saving method that significantly reduces energy costs [7]. The main principle involves using outside air or water as the cooling medium or direct cooling source for DCs [8], thereby replacing traditional systems like air conditioning [9]. Due to its advantages in energy conservation, environmental protection, low operation and maintenance costs, and support for sustainable development, this technology has been widely adopted in industrial production, building air conditioning systems, and electronic equipment heat dissipation. Endo et al. [10] conducted a one-year operational test with a container DC in the suburbs of Tokyo, demonstrating that direct fresh air cooling could save 20.8 % of energy annually compared to traditional air conditioning, with a power usage effectiveness (PUE) as low as 1.058.

Chen et al. [11] proposed a two-stage chip-level cooling system without pumps and water, achieving an annual PUE reduction to 1.15 in Beijing, thereby significantly reducing the total energy consumption of DC by 30 %. This provides a direction for realizing the year-round natural cooling in most of regions in China. Zhang et al. [12] monitored rack temperatures in a natural air-cooled fan-wall DC model and monitored temperature fluctuations, evaluating airflow organization using the SHI index, they found that arranging fans in a single-column fan-wall configuration could reduce the average heating index by up to 54.1 %. From previous literature, it is evident that there is significant potential for applying natural cooling technology in DC cooling systems. However, relying solely on natural air cooling for DC cooling has the drawback of lower cooling efficiency. Moreover, only a few regions experience meteorological conditions conducive to utilizing outdoor fresh air for natural cooling throughout an extended period of the year.

Evaporative cooling is an environmentally friendly and cost-effective cooling technology [13]. It operates by extracting heat from the air through the evaporation of water molecules, converting the heat into latent heat to achieve cooling [14]. Cui et al. [15] evaluated the natural cooling potential of indirect evaporative cooling by analyzing various operation modes and confirmed the feasibility of evaporative cooling technology in DCs. Lv et al. [16] proposed a multi-combination evaporative cooling-dehumidification air conditioner with multiple operation modes according to the characteristics of different climates and humidity levels. Their study explored the effects of ambient temperature and humidity on cooling efficiency, refrigeration capacity, and performance coefficient, demonstrating a 55.9 % increase in performance coefficient compared to traditional compression refrigeration air conditioner. Hnayno et al. [17] conducted an experimental study on temperature differential cooling optimization in DCs using an indirect natural cooling system equipped with evaporative cooling pads. They found that pre-cooling the water supply prior to the dry cooler operation could reduce cooling demand by at least 31 %. However, despite its efficient cooling capabilities, evaporative cooling technology still faces potential challenges related to humidity control.

Phase change energy storage (PCES) is characterized by high energy density, large latent heat, and long service life [18]. It stores energy by releasing or absorbing latent heat during the phase transition of materials [19]. Phase change materials (PCMs), as efficient and durable energy storage mediums, can ensure the reliable operation of green DCs [20]. Huang et al. [21] developed a PCM-based cooling storage unit for emergency cooling in air-cooled modular DCs, conducting experiments on its charge and discharge process. They demonstrated that the PCM unit could meet emergency cooling demands for at least 5 minutes, with the addition of curved fins extending this duration by 42 seconds and reducing charging time by 1850 seconds. Yuan et al. [22] utilized liquid paraffin as PCM and various inorganic copolymers as a flexible matrix, optimizing size, thermal conductivity, and enthalpy values using Flotherm software. Their results showed that paraffin could reduce the temperature by over 10℃ and extended safe temperature durations during emergencies. Ljungdahl et al.[23] employed Matlab to develop a decision model integrating latent heat storage with liquid cooling technology to recover waste heat resource in DCs. Their analysis indicated that implementing this supplementary operation system configuration as a local heat source in Denmark could achieve energy savings of 332 % annually. Research on PCM in DCs has primarily focused on emergency cooling [24] or waste heat recovery, with limited exploration into continuous cooling applications within computer rooms. Overall, previous studies predominantly examined the feasibility of individual technologies such as natural cooling, evaporative cooling, or PCES for constructing temperature control systems in green DC. There remains little research on the simultaneous utilization of all three technologies for DC cooling systems.

Addressing the challenge of prolonged cooling for air supply in DCs under high-temperature meteorological environments, this paper proposes a novel DC cooling system integrating three technologies: air-cooled free cooling, direct evaporative cooling (DEC), and PCES. Based on the meteorological characteristics of Gui'an New Area, Guizhou Province, these technologies are combined to manage the temperature and humidity of outdoor fresh air. This study aims to verify the feasibility and effectiveness of this integrated cooling system in achieving efficient cooling in medium-high temperature environments through simulations under various fresh air conditions. The effects of several control factors such as inlet air temperature, inlet speed, inlet humidity, and spray flow on the cooling performance of the ventilation system are analyzed systematically. Furthermore, the main and secondary factors affecting the refrigeration performance of the integrated cooling system are studied by orthogonal experiments. The research provides insights for enhancing DC cooling systems and lays groundwork for optimizing PCM and DEC devices in future studies.

2. Methodology

2.1 Experimental program

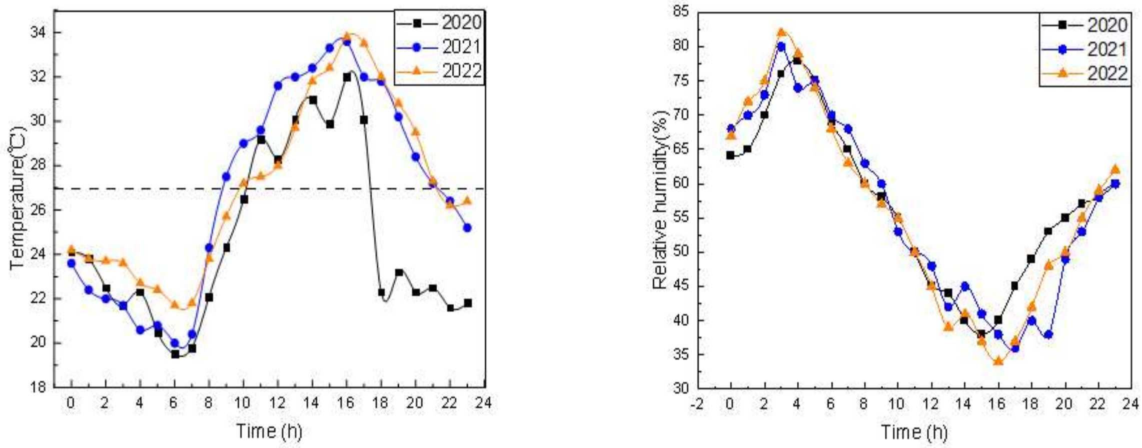

(a) The full-time temperature of the highest day in year (b) Relative humidity changes during the hottest day

Fig. 1. Air temperature and humidity in Gui'an New District, Guiyang, 2020-2022

Fig. 1 illustrates the variation in temperature and relative humidity during the hottest days in Gui'an New District, Guiyang City, Guizhou Province, China, from 2020 to 2022. From Fig. 1(a), the external air temperature exceeded 27 °C for 7, 13 and 12 hours, respectively, over the past three years. Fig. 1(b) indicates that outdoor relative humidity is generally higher at night compared to daytime. When combined with the data from Fig. 1(a), the average relative humidity during daytime hours with temperatures above 27°C is 43.1%, 45.6%, and 44.4% for the years 2020, 2021, and 2022, respectively. Therefore, it is essential to address these high temperature and moisture meteorological conditions to ensure a safe and low-temperature air supply for DCs.

Furthermore, from Fig. 1(a), it can be observed that the maximum temperature reached on the hottest day was 32 °C in 2020, with an average diurnal-nocturnal temperature difference of 5.2 °C. In 2021, the maximum temperature rose to 33.6 °C, accompanied by a diurnal-nocturnal temperature difference of approximately 7.7 °C. Similarly, in 2022, the maximum temperature recorded was 33.8 °C, with a day-night average temperature difference of about 5.69 °C. To address these conditions, DEC can effectively provide high-efficiency cooling, while the significant daily temperature difference offers potential for PCES. Therefore, we propose an integrated ventilation system that combines evaporative cooling with PCES under natural air-cooling conditions.

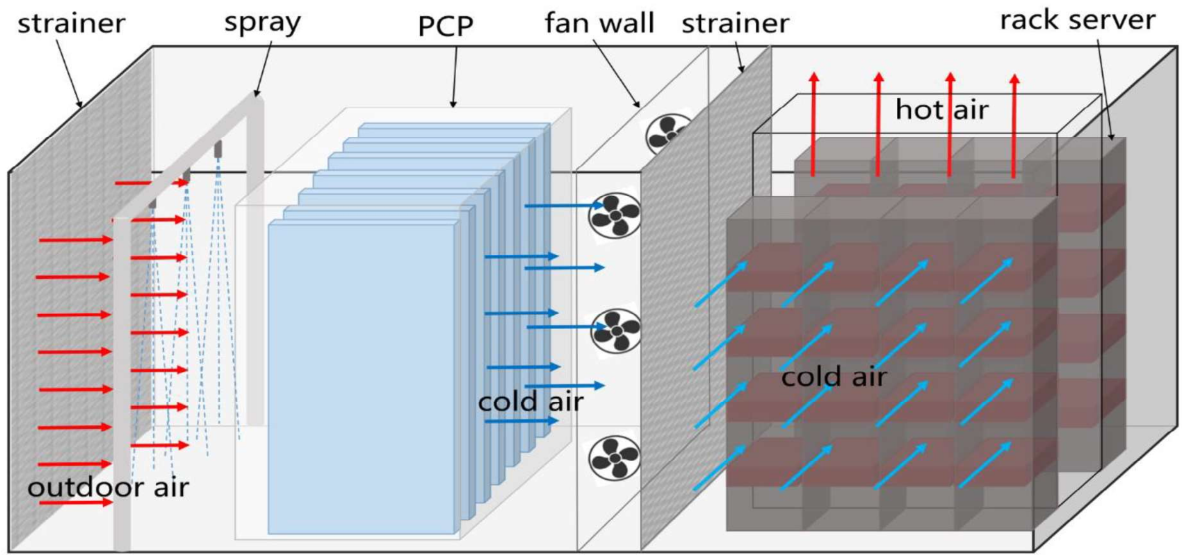

Fig. 2. Evaporative cooling coupled PCES ventilation schematic diagram

In this study, DEC and PCES are utilized for the treatment of temperature and humidity in outdoor fresh air. The spray room functions as the direct evaporative cooler [26]. After undergoing primary treatments such as purification and filtration, outdoor fresh air is directed into the refrigeration channel where it interacts directly with water in the spray room. Here, the air comes into contact with a saturated layer of water molecules on the outer surface, causing evaporation or condensation due to differences in vapor pressure between the water molecules and the surrounding air [27], facilitating heat and humidity exchange [28]. The difference between the dry bulb temperature and the wet bulb temperature determines the maximum temperature reduction achievable through DEC [29]. Then the air flows through the Phase change plates (PCP) section where PCM is encapsulated in a metal plate indirectly interacting with the air [30]. This setup facilitates heat exchange and energy transfer simultaneously[31], enabling further temperature and humidity treatment of the air. Finally, the conditioned air meeting the air supply requirements is circulated to the machine for cooling treatment. The integrated evaporative cooling coupled with PCES ventilation system under natural air cooling conditions is shown in Fig. 2.

2.2 Experimental platform construction

The experiment was conducted in the artificial environment lab in Guizhou University, Guizhou Province, China, as shown in Fig. 3(a). The artificial environment laboratory measures 6.7 m in length, 3.1 m in width, and 3 m in height. It comprises a ventilated room of 3.6 m in length, 3.1 m in width, and 3 m in height, as well as a cooling room of 3.1 m in length, 2 m in width, and 3 m in height. These two rooms are connected by a window measuring 1.1 m in length and 0.9 m in width. The air handling system includes a ventilation channel that is 2 m in length, 0.65 m in width, 0.65 m in height, and 5 mm thick, made of transparent acrylic. This system features a spray section and a phase change section. Different fresh air conditions, matching the meteorological characteristics of Gui'an New Area in Guizhou, are simulated through a control platform located outside the artificial environment room. To prevent outdoor airflow interference and heat loss, the windows of the artificial environment room, and the part not directly connected to the ventilation channel, are sealed with 3 cm thick insulation cotton. However, one air inlet, one connecting window, and one section connected to the channel are not sealed.

The principle of the experimental process is illustrated in Fig. 3(b). During the heating air supply process, the fresh air is initially drawn into the handing units by a fan. It is then adjusted to the required temperature via the control platform and conveyed into the ventilation room through the air supply duct. The heated air, assisted by a fan wall composed of 20 small fans, passes through the spray section and the PCP section for successive temperature and humidity treatment. Furthermore, for the cooling air supply process, the main objective is to solidify PCM. Cold air is blown into the cooling room by switching on the cooler to simulate the nighttime atmospheric conditions. This cold air is then sent back into the integrated cooling channel through the window connecting the ventilation room, guided by the fan, to solidify the PCM. The cooling channel consists of two parts: the spray section and the PCM section.

(a) Experimental platform

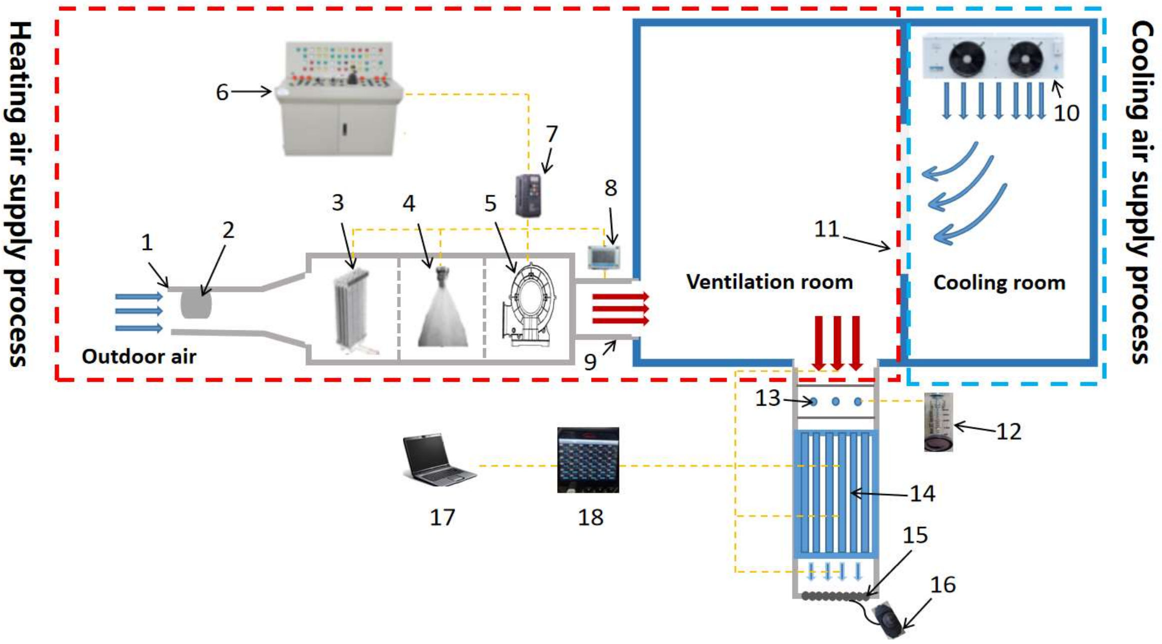

1.Air handling units 2. Exhaust fan 3. Heating section 4. Spray section 5. Fan
6. Console platform 7. Frequency converters 8. Velocity transmitter 9. Air supply ducts
10. Air cooler 11. Windows 12. Flowmeter 13. Nozzles 14.PCP 15. Fan wall
16. Speed regulation line 17. Computer 18. Data acquisition instrument

(b) Principle of experiment

Fig. 3. Experimental platform and schematic diagram of integrated cooling system

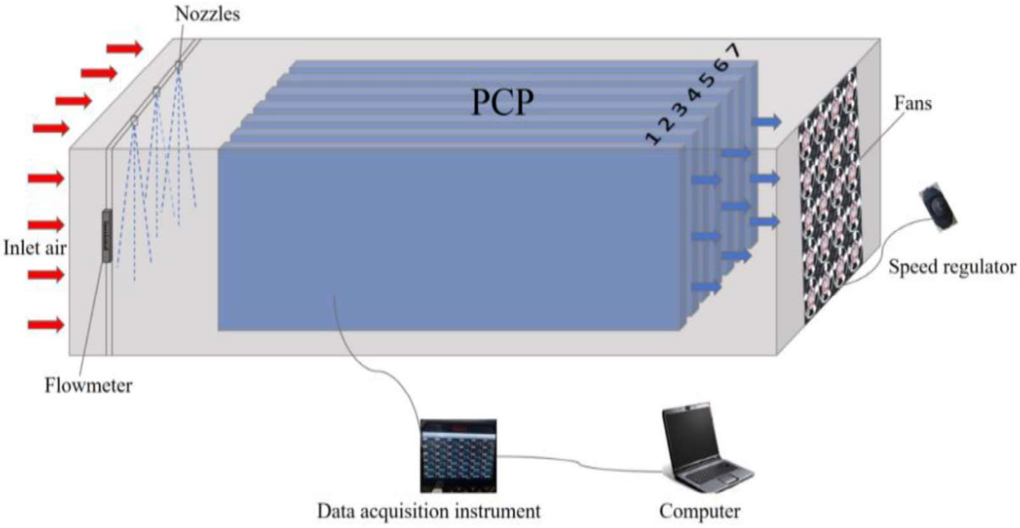

Fig. 4. Schematic diagram of integrated cooling system

The structure of the cooling system is shown in Fig. 4. It includes three nozzles with a hole diameter of 0.35 mm, constructed from nickel-plated copper in the spray section. The PCP dimensions are 1.15 m (L) × 0.59 m (W) with a thickness of 2 cm, filled with paraffin and encased in a 1 mm thick tin-plated shell. Experimental data acquisition is conducted with a scanning rate of 2 minutes per session, using PT1000 thermocouples, a data collector, fan, fan linear speed line, anemometer, flow meter, water pump, temperature and humidity sensors, as illustrated in Fig. 5. Key technical parameters are summarized in Table. 1.




(a)Data collector **(b)Hygrometer** **(c)Impeller-type anemometer** **(d)Fan**




(e)Humidifier **(f)Thermocouple** **(g)Rotameter** **(h)pump**

Fig. 5. Main experimental instrument

Table 1. Main design parameters of equipment

Equipment name	Equipment type	Uncertainty	Range	Remark
Temperature collector	MIK-6000F	Read value × 0.5% + 1 °C	-200 - 800°C	Work environment: 20 - 90%
Thermocouple	Pt1000	± 0.01°C	-50 - 200°C	Length of the line: 3 m
Rotameter	DFG-6T	±4%	40-400 ml/min	Screw thread: M18×1.5 G1/4’’ 1/4’’BSP
Water pump	Diaphragm pump	/	60 w	Theoretical head: 50m Suction height: ≤1.5m
Fans	SF8025ATa	± 0.05 m^3/min	2 m^3/min	Work environment: -10 - 60 °C
Impeller-type anemometer	FLUKE-925	Full scale ± 2%	0.40 - 5.00 m/s	Work environment: 0 - 50 °C
Humidifier	XH-806C	± 2%	6 kg/h	/
Hygrometer	ZL-TH10TP	± 3%	0-99%RH	Work environment: -20-50 °C

2.3 Experimental material

Recently, PCM have been widely used as latent heat storage [32]. Commonly classified into eutectic, inorganic, and organic types [33], PCM are valued for their high energy storage density and ability to operate with low temperature difference [34]. Paraffin, as an organic PCM, exhibits good thermal properties, stable chemical characteristics, and resistance to phase separation [35]. In this study, paraffin with a phase change temperature range of 23-25 °C is employed as the PCM. Taking advantage of its heat absorption and release capabilities during phase change [36], the PCM solidifies naturally during cooler nighttime temperatures [37]. As daytime temperature rise, the PCM, enclosed within a 1 mm thick tin-plated shell that indirectly contacts the air, undergoes heat exchange, absorbing heat from the air and gradually transitioning to a liquid state [38]. This process effectively cools the air. The thermophysical properties of paraffin were analyzed using differential scanning calorimetry. The resulting curve is displayed in Fig. 6. More specific melting and solidification characteristics of paraffin are detailed in Table. 2 and illustrated in Fig. 7.

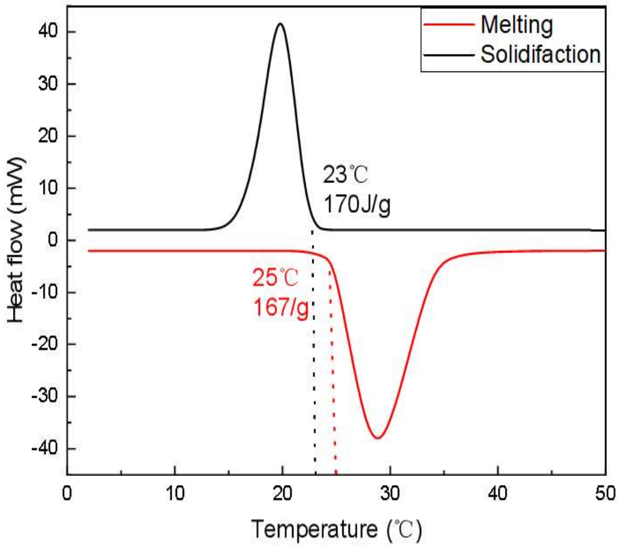

Fig. 6. The differential scanning calorimetry test result of paraffin.

Table 2. The specific of paraffin

Parameters	**Counts**
Starting temperature of melting (°C)	25°C
Starting temperature of solidification (°C)	23°C
Density of liquid(kg/m^3)	880
Density of solid(kg/m^3)	850
Thermal conductivity (W/(m·K))	0.21
Latent heat (kJ/kg)	167/170
Specific heat (kJ/(kg·K))	3.12-3.34
Flashing point(°C)	> 250°C
Maximum working point(°C)	200°C

(a) The state of solid paraffin at 15 ℃ **(b) The state of liquid paraffin at 35 ℃**

Fig. 7. Melting and solidification diagram of paraffin

2.4 Measure point arrangement

At the entrance of the cooling device, located 50 cm from the air inlet after spraying and 5 cm from the outlet, see Fig. 8(a), four temperature measurement points are positioned. Additionally, at the center of each of three cross-sections (as shown in Fig. 8(b)), one humidity measurement point is established to observe and record the changes in temperature and humidity of the air after passing through different stages. Within the middle section of the 7 PCP units (depicted in Fig. 8(c)), four temperature measurement points are placed to monitor the temperature changes of the PCM. To ensure accuracy, each temperature measurement point utilizes a PT1000 thermocouple, and the data is recorded and stored using an MIK-6000F paperless recorder. The three humidity measurement points are monitored by a ZL-TH10TP temperature and humidity detector, which also records and saves data electronically.

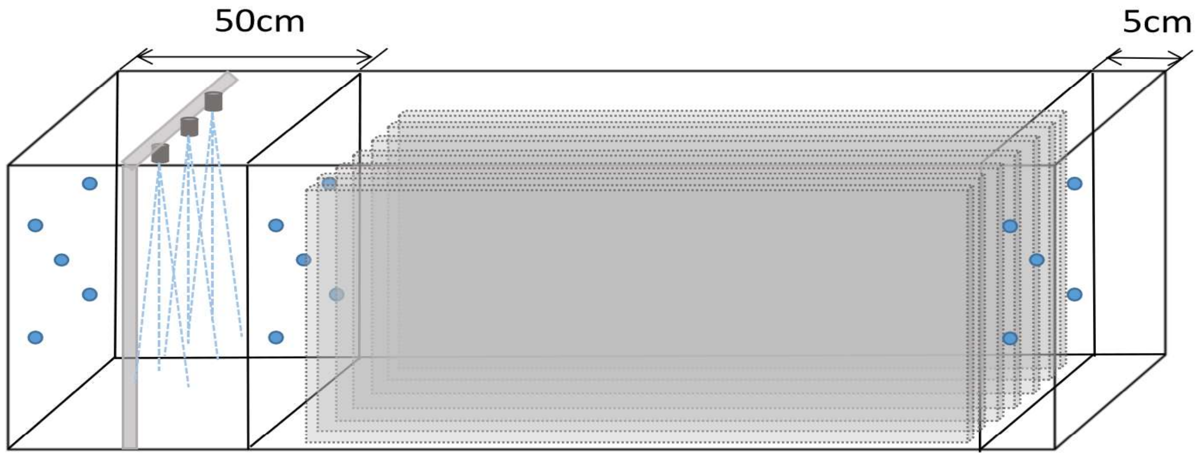

(a) Measurement points in three cross-sections

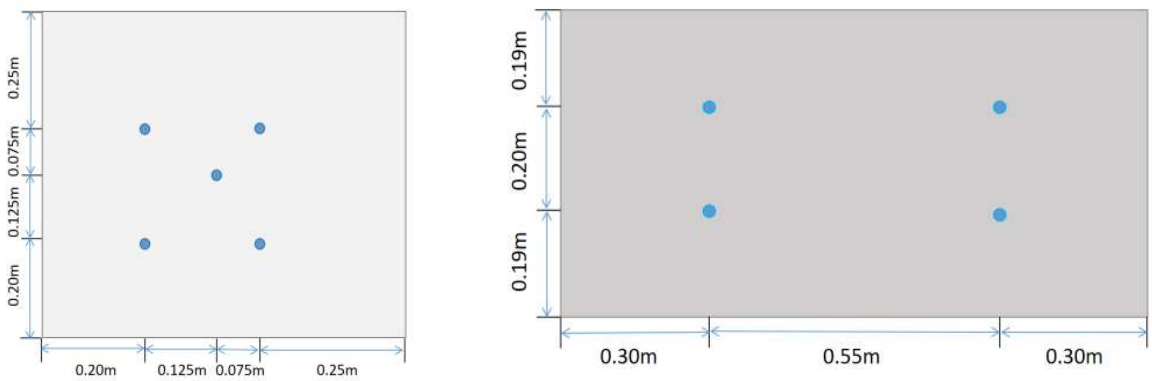

(b) Air temperature and humidity measurement points (c) Measurement points inside the PCP

Fig. 8. Distribution of temperature and humidity measurement points

2.5 Working condition design

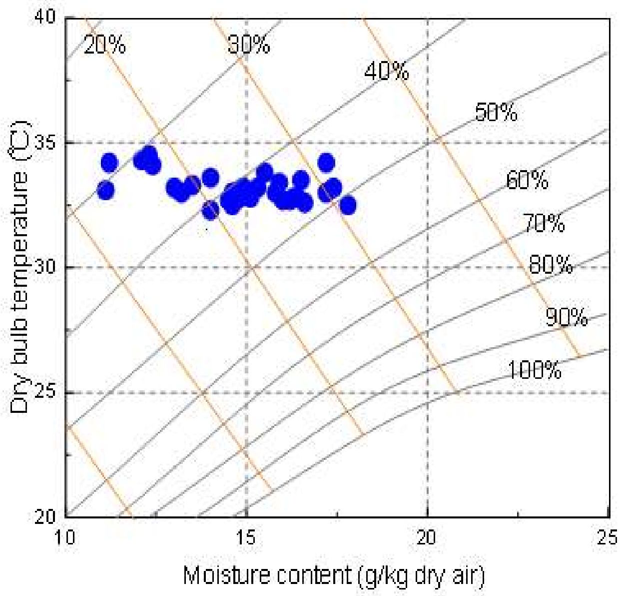

Fig. 9. Enthalpy-humidity diagram of Guiyang New District during temperature above 32 °C in 2020-2022

In this study, meteorological data from Gui'an New Area in Guizhou Province were taken as an example. Daily temperature and humidity measurements were collected from 2020 to 2022. The maximum values of temperature and humidity at each moment of the day throughout the year were monitored and recorded. Specifically, statistics were gathered for days with high temperatures of 32℃ and above during this period. As shown in Fig. 9, during the past three years, relative humidity reached approximately 40% on two-thirds of these high-temperature days, with a maximum temperature of 34.8℃ and a maximum relative humidity of 50.8%.

Therefore, the effects of several control factors such as inlet air temperature, inlet speed, inlet humidity and spray flow on the overall cooling performance of the cooling system were experimentally investigated. The methodology employed controlled variables where one parameter was varied while keeping others constant. Each factor was tested at four levels using a one-way analysis approach. The experimental conditions included are: inlet air temperatures of 28 °C, 30 °C, 32 °C, 34 °C; inlet velocities of 1 m/s, 1.5 m/s, 2 m/s, 2.5 m/s; inlet humidity of 30 %, 35 %, 40 %, 45 %; spray flows of 0.04 L/min, 0.06 L/min, 0.08 L/min, 1 L/min. Detailed experimental design specifics are provided in Table 3.

Table 3. Working condition design

Case	Inlet temperature (°C)	Inlet speed (m/s)	Inlet humidity (%)	Spray flow (L/min)
1	**28**	1.5	30	0.08
2	**30**	1.5	30	0.08
3	**32**	**1.5**	**30**	**0.08**
4	**34**	1.5	30	0.08
5	32	**1**	30	0.08
6	32	**2**	30	0.08
7	32	**2.5**	30	0.08
8	32	1.5	**35**	0.08
9	32	1.5	**40**	0.08
10	32	1.5	**45**	0.08
11	32	1.5	30	**0.04**
12	32	1.5	30	**0.06**
13	32	1.5	30	**0.1**

2.6 Experimental steps

Take experiment case 1 as an example, the experimental steps are as follows:

(1) Fix 7 PCP containing completely solid paraffin in the ventilation channel by means of the special wooden frame.

(2) Set the recording interval of the paperless recorder to 2 min.

(3) Open the air cooler to blow cold air into the ventilation room, inducing cooling curing of the PCM.

(4) Switch off the cooler, turn on the console platform, controlling the inlet temperature at 28 ± 0.5 °C.

(5) Turn on the humidity regulator, control the relative humidity in ventilation room at 30 ± 2 %.

(6) Open the pump, adjust the rotameter, control the spray flow at 0.08 ± 0.005 L/min.

(7) Set the fan on, modulate the wind speed regulator, set the inlet speed at 1.5 ± 0.3 m/s.

(8) Maintain stable operation for 8 h, record the data by paperless recorder.

(9) Repeat the above experimental steps, change the parameters according to the set working conditions, until all test cases are complete.

2.7 Experimental uncertainty

The uncertainty of the measured variable is mainly the uncertainty of the measuring instrument

[39]. Analysis multiple measurements can reduce data inaccuracies [40]. The uncertainty analysis of the instrument is carried out using the famous Bessel formula [41].

The sample variance is known to be:

$$S_{\sigma}^{2}=\frac{1}{n-1}\sum_{i=1}^{n}(x_i-\bar{x})^2=\frac{1}{n-1}\sum_{i=1}^{n}v_i^2 \quad (1)$$

If the standard deviation of the sample is used as an estimate of the standard deviation:

$$\hat{\sigma}=S_{\sigma}=\sqrt{\frac{1}{n-1}\sum_{i=1}^{n}\left(x_i-\bar{x}\right)^2}=\sqrt{\frac{1}{n-1}\sum_{i=1}^{n}v_i^2} \quad n>1. \quad (2)$$

Where, n is the number of measurements; $v_i$is the residual of the I-th measurement; x_i is the measurement value obtained from the ith measurement, i=1, 2, 3 ......, n; $\bar{x}$ is the arithmetic mean of n measurements.

3. Results

3.1 Cooling performance of PCP

The experimental conditions were as follows: inlet air speed of 1.5 m/s, inlet temperature of 32 °C, inlet humidity of 30 %, and spray flow of 0.08 L/min. Seven PCM plates, labeled from Plate 1 to Plate 7 from left to right, were monitored for real-time temperature measurement using a data acquisition instrument. Ventilation 8 h within the melting of PCM, material temperature changes, as well as the changes in inlet and outlet air temperature and humidity are shown in Fig. 10.

(a)Experiment started 0 h

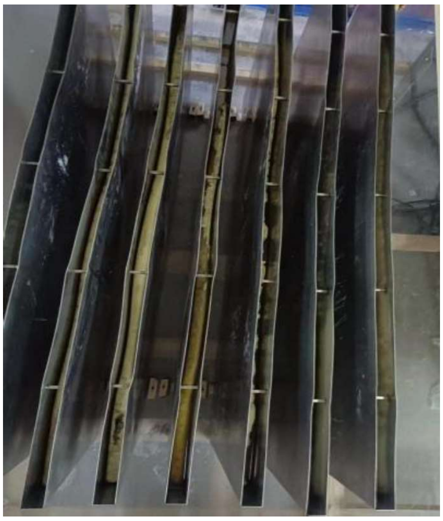

(b)Experiment started 2 h

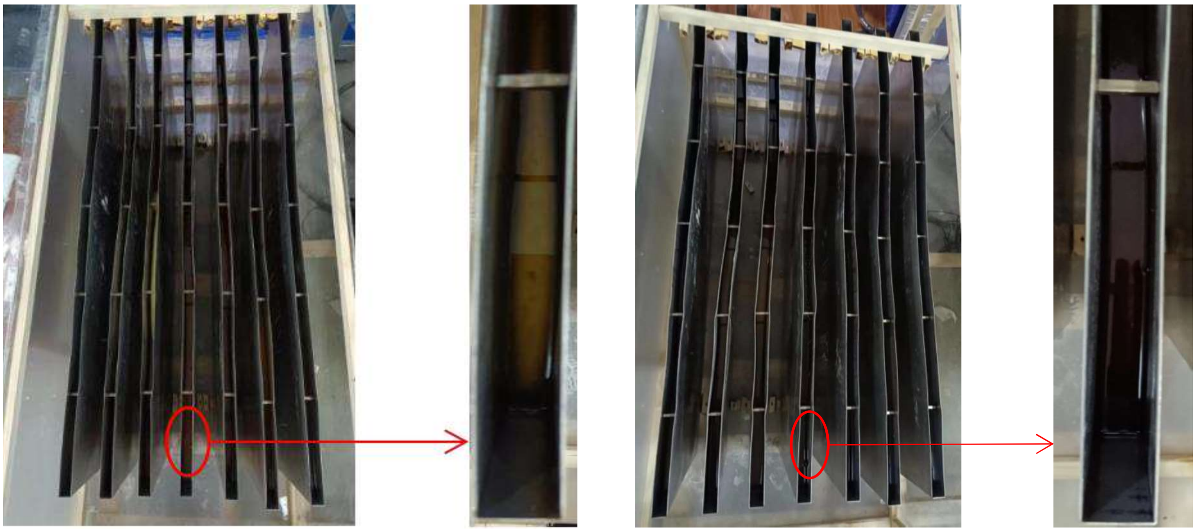

(c)Experiment started 4 h **(d)Experiment started 8 h**

Fig. 10. Melting of PCM within 8 h

As depicted in Fig. 9, as the experiment progressed, the paraffin absorbed heat from the air flowing through the channel, gradually transitioning from a solid to a liquid state. The phase change temperature range of the paraffin used in this experiment is 23-25 °C. During the initial 2 hours of the experiment, the temperature of the paraffin increased most rapidly when it was predominantly in a solid state. Between 2-4 hours, the paraffin began to melt, resulting in a slower rate of temperature increase. Initially, the outer shell of the PCP section started melting first. Beyond 4 hours, the temperature of the paraffin increased gently, indicating a trend towards stabilization, with most of the paraffin having melted by this stage. By then end of 8 hours, the paraffin had largely melted and transformed into a liquid state.

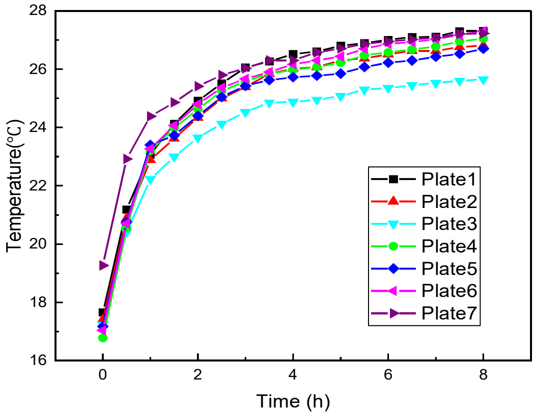

Fig. 11. Temperature variation of in PCP

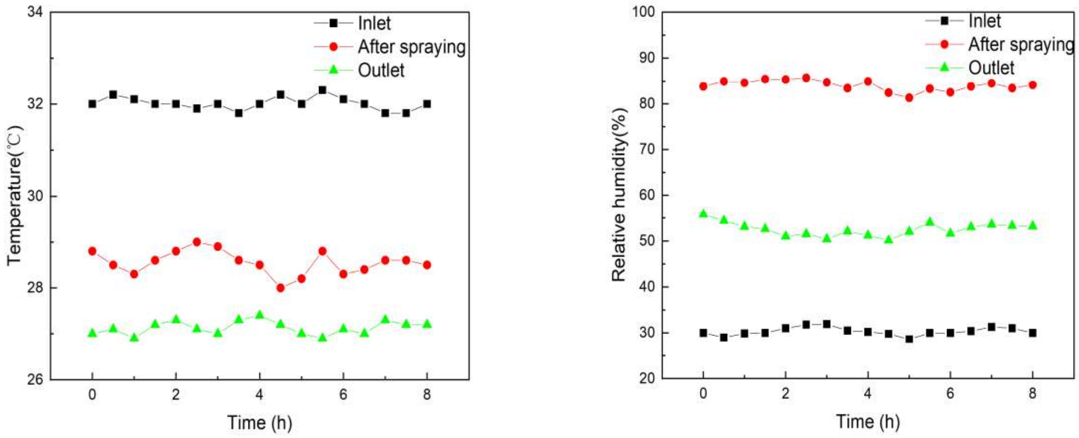

(a) Changes in temperature **(b) Changes in relative humidity**

Fig. 12. Changes in inlet, post-sprinkler and outlet air temperature and humid

Fig. 11 shows a gradual increase in the temperature of paraffin over time, stabilizing after approximately 4 hours. Plate 3 exhibits a lower temperature compared to other PCP plates due to the instability and uneven distribution of air circulation, which results in insufficient contact between the air and the PCP, thereby limiting heat exchange.

As can be seen from Fig. 12, after spraying, the maximum temperature drop of about 5 ℃ is achieved, accompanied by high humidity around 85 %. Subsequently passing through the PCP, the outlet air temperature stabilizes at approximately 27 ℃, with a relative humidity of about 55 %. These findings indicate that evaporative cooling predominantly influences the cooling effectiveness of the integrated cooling system, achieving a maximum temperature drop of 5 ℃. On average, the temperature decreases by approximately 1.3 ℃ after passing through the PCP segment.

Furthermore, upon comparing the relative humidity of the air after spraying and at the outlet, it can be noticed that the humidity of the air is approximately 35 % lower after passing through PCP. This reduction occurs because as the air flows through the PCP section, it collides with the shell, leaving behind tiny liquid droplets on the metal surface. Moreover, due to the higher temperature of the air compared to the PCP in the initial periods, water vapor condenses upon contact with the cooler surfaces, residual in the PCP metal shell surface, as the experiment proceeds, the temperature of paraffin increases gradually, the difference between air and PCP decreases, thus the condensation phenomenon is gradually weakened.

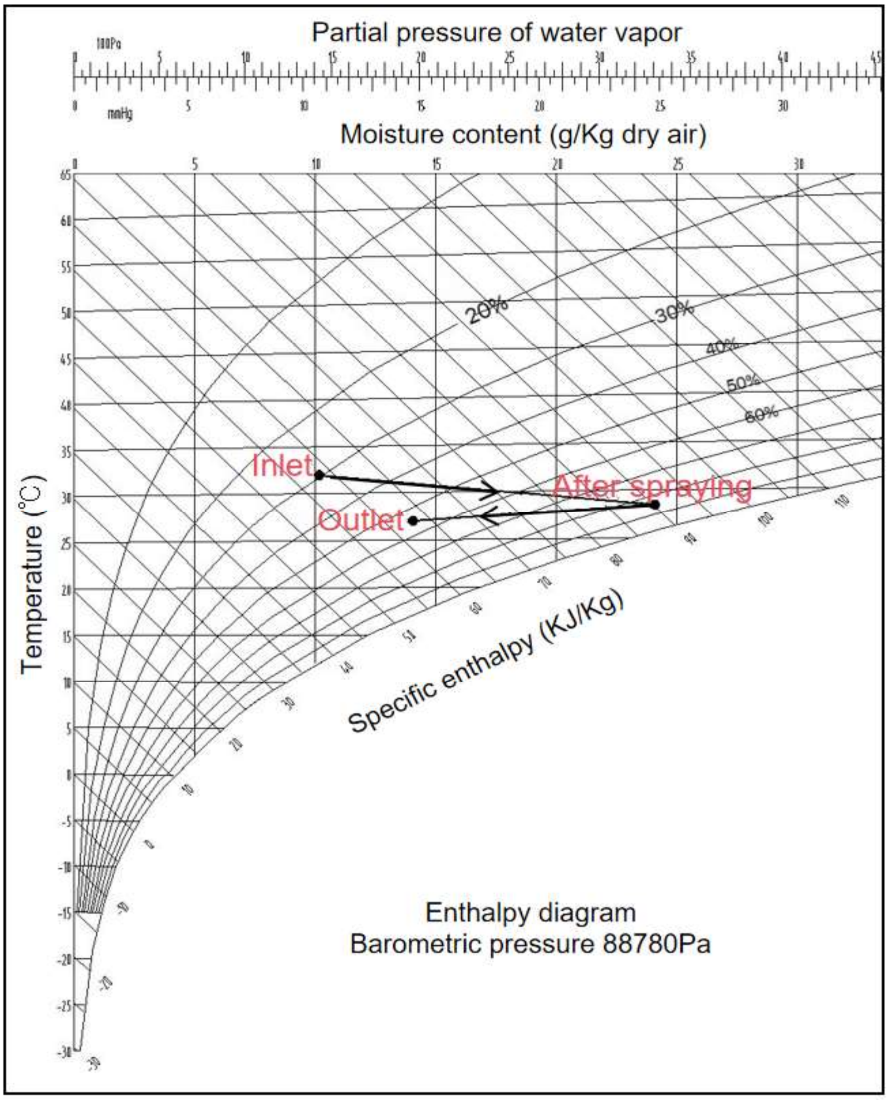

Fig. 13. Enthalpy-humidity diagram of air circulation process

Taking the atmospheric pressure of the Guiyang area in Guizhou, China as a baseline, and combining it with experimental data on temperature and relative humidity at the inlet, after spraying, and outlet as shown in Fig. 12, the process of enthalpy and humidity change for air passing through the device is plotted, as shown in Fig. 13. By averaging the data over an 8-hour working period, it can be observed that the entire process from start to finish is close to an isenthalpic cooling and humidification process. But due to the instability of air flow, the heat loss during the heat and moisture exchange between paraffin wax and water and air, such as part of the water droplets are not in complete contact with the air, the heat absorbed by the metal shell wrapped around the paraffin in the process, etc., resulting in a certain gap with the ideal state of isenthalpic cooling and humidification process, the whole process is a cooling and humidifying process.

The feasibility and high efficiency of evaporative cooling combined with PCES technology are confirmed based on the melting behavior of the PCM and the observed changes in air temperature and humidity at each measurement point.

3.2 Multi-factor sensitivity analysis

3.2.1 Effect of inlet temperature

The experimental conditions are set as follows: an air inlet speed of 1.5 m/s, a spray flow rate of 0.08 L/min, an inlet humidity of 30 %, and varying inlet air temperatures of 28 °C, 30 °C, 32 °C, 34 °C, respectively. The changes in temperature and humidity of the air at different inlet temperatures after each stage of treatment are shown in Figs. 14 and 15.

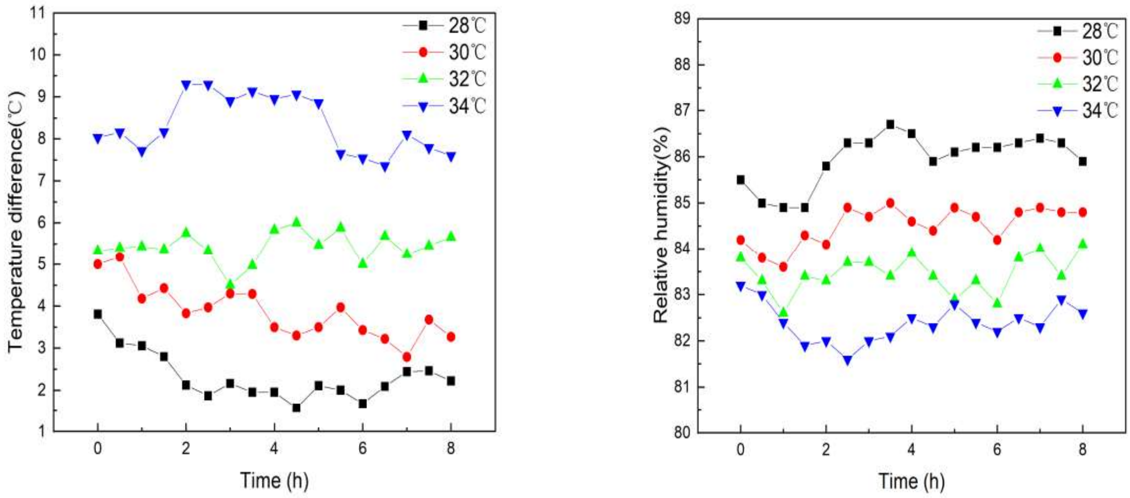

(a)Temperature difference between spray and inlet **(b) Relative humidity after spraying**

Fig. 14. The change of temperature and humidity after spraying

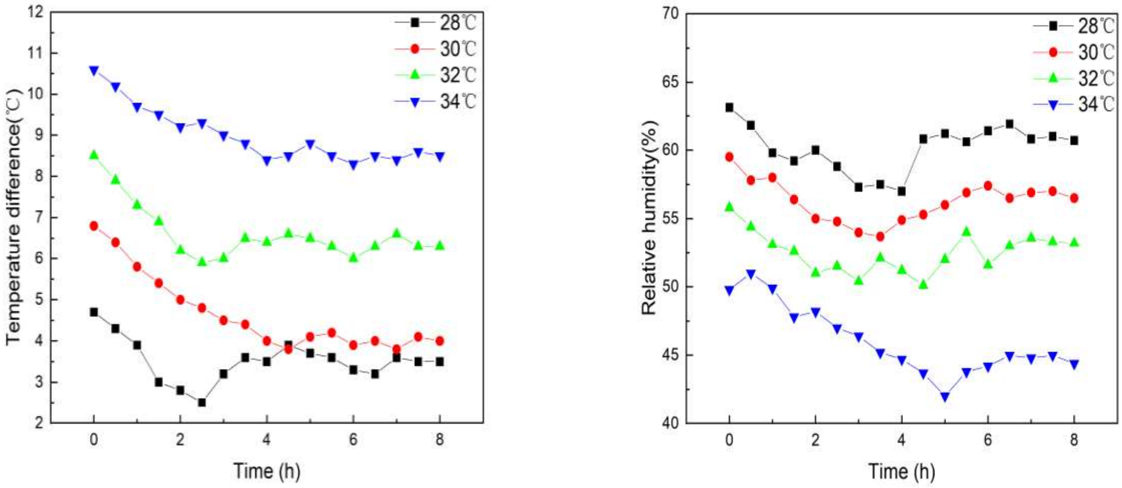

(a) Temperature difference between outlet and inlet **(b) Outlet relative humidity**

Fig. 15. The change of temperature and humidity at the outlet

From Fig. 14(a) and Fig. 15(a), it is observed that the maximum temperature reduction achievable after spraying is 3.8 °C, 5 °C, 5.75 °C, and 9.3 °C for inlet air temperatures of 28 °C, 30 °C, 32 °C, and 34 °C, respectively. The maximum temperature drop between the outlet and the inlet air is 4.7 °C, 6.8 °C, 8.5 °C, and 10.6 °C, indicating that the cooling performance of the integrated cooling system is primarily driven by evaporative cooling. In the PCP section, a temperature drop of 0.6 °C to 2.75 °C is achieved. Observing Fig. 14(b) and Fig. 15(b), the relative humidity of the air after spraying is maintained between 81% to 87%, which does not reach the absolute saturation due to environmental factors such as insufficient air-water contact time, inadequate water volume, and air turbulence. After passing through the PCP, the humidity is maintained between 40 % and 65 %, demonstrating that the PCP can reduce humidity by 22 % to 41 %. During the cycle through the PCP section, the air with high moisture content comes into direct contact with the PCP's metal shell. As a result of this contact and collisions, some water vapor remains on the PCP shell. Moreover, due to the temperature difference between the air and the PCP, condensation occurs, effectively lowering the air humidity.

In summary, with the increase of the inlet air temperature, the cooling performance of the integrated cooling system improves gradually. The maximum temperature drop is achieved when the air temperature reaches 34 °C. Furthermore, the phase transition latent heat exchange section of the integrated cooling system not only facilitates cooling but also effectively reduces humidity. Therefore, for regions like Guizhou and other areas with high temperatures, high humidity or low humidity areas, evaporative cooling coupled with PCES technology under natural air cooling shows significant potential for practical application.

3.2.2 Effect of inlet speed

Experimental conditions were set as follows: inlet temperature of 32 ℃, spray flow of 0.08 L/min, inlet humidity of 30 %, and inlet air speeds controlled at 1 m/s, 1.5 m/s, 2 m/s, and 2.5 m/s by adjusting the linear transmission of the fan. The temperature and humidity changes of the air after treatment at different inlet air speeds are shown in Figs. 16 and 17.

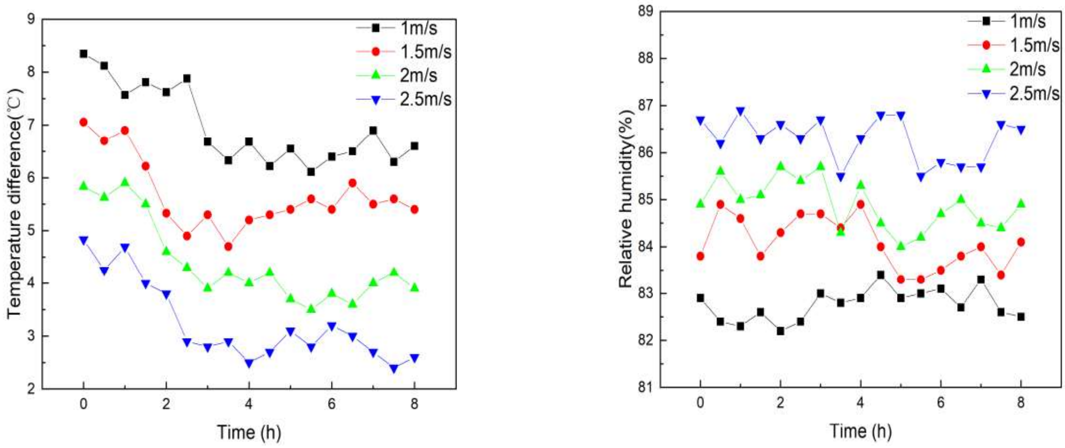

(a)Temperature difference between spray and inlet **(b) Relative humidity after spraying**

Fig. 16. The change of temperature and humidity after spraying

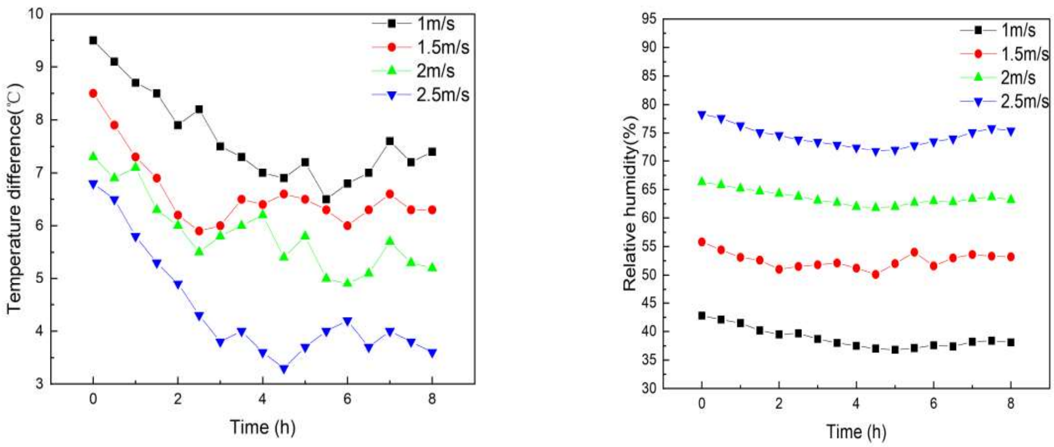

(a) Temperature difference between outlet and inlet **(b) Outlet relative humidity**

Fig. 17. The change of temperature and humidity at the outlet

As shown in Fig. 16(a) and Fig. 17(a), under different inlet air speeds, the overall air temperature difference initially decreases and then stabilizes. When the wind speed is 1 m/s, spraying can achieve a maximum temperature reduction of 8.3 °C and a minimum of 6.3 °C. After passing through the PCP, the maximum temperature reduction compared to the inlet is 9.5 °C, and the minimum is 6.5 °C. The integrated cooling system performs best at an inlet speed of 1 m/s. This is because, as the wind speed increases, the contact time between the air, water, and PCM becomes shorter, leading to insufficient heat exchange and deteriorating cooling performance. Fig. 16(b) and Fig. 17(b) indicate that, due to the instability and non-uniformity of spray flow and airflow, the relative humidity after spraying remains in the range of 78 %-88 %, achieving humidification of 48 %-58 %. After passing through the PCP, the outlet air humidity stabilizes at approximately 40 %, 55 %, 65 %, and 78 %, meeting the air supply requirements for DCs. In summary, the system achieves the best cooling performance at an inlet speed of 1 m/s.

3.2.3 Effect of inlet humidity

Experimental conditions were set as follows: inlet temperature at 32 °C, inlet velocity at 1.5 m/s, spray flow at 0.08 L/min, and the humidity in the ventilation room is controlled by adjusting the humidifier to be 30 %, 35 %, 40 %, and 45 %, respectively. The changes in temperature and humidity of the air after each stage of treatment under varying inlet air humidity conditions are depicted in Figs. 18 and 19.

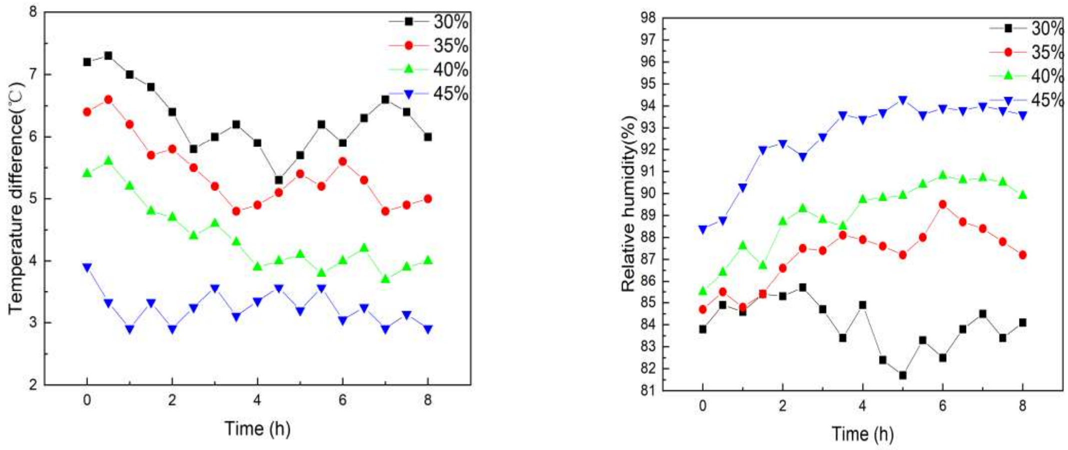

(a)Temperature difference between spray and inlet **(b) Relative humidity after spraying**

Fig. 18 The change of temperature and humidity after spraying

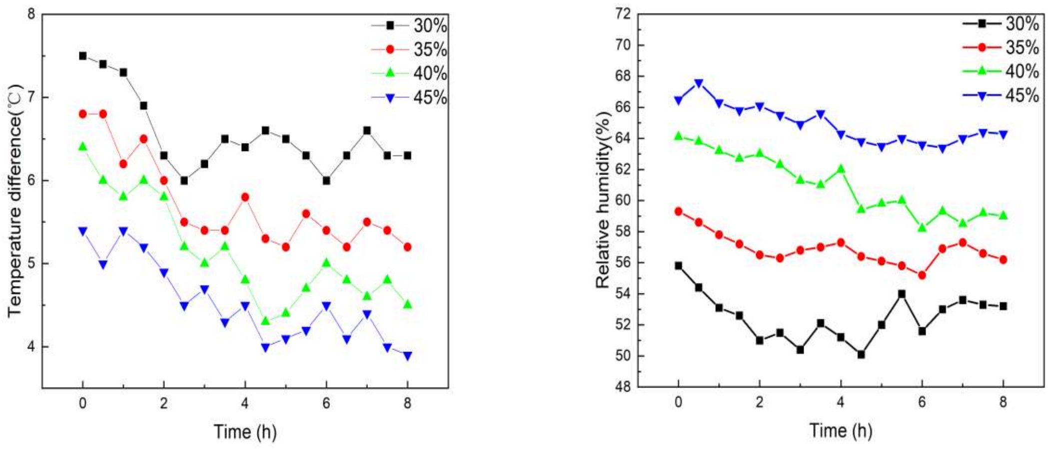

(a) Temperature difference between outlet and inlet **(b) Outlet relative humidity**

Fig. 19 The change of temperature and humidity at the outlet

As shown in Fig. 18(a) and Fig. 19(a), the cooling performance gradually decreases with the increase of the inlet air humidity. When the inlet humidity reaches 45 %, the maximum temperature drop achieved after spraying is 3.9 ℃. Passing through the PCP, a maximum temperature drop of 5.4 ℃ can be achieved compared to the inlet air temperature. This is because, as the moisture content of the air increases, the latent heat exchange generated by water evaporation decreases during direct contact between air and water, and sensible heat exchange becomes dominant. Consequently, the cooling effect achievable through the DEC process is relatively reduced, leading to a worse cooling performance of the system. Fig. 18(b) and Fig. 19(b) illustrate that the relative humidity of the air at each stage increases with the increase of the inlet air humidity. At an inlet humidity of 45 %, the maximum outlet air humidity is 68 %. The PCP can achieve a moisture reduction of 25 %-35 % compared to the inlet humidity. Overall, the system performs best when the inlet air humidity is 30 %.

3.2.4 Effect of spray flow

Experimental conditions were set as follows: inlet temperature at 32 ℃, inlet speed at 1.5 m/s, inlet humidity at 30 %, and spray flow is controlled by adjusting the rotameter to 0.04 L/min, 0.06 L/min, 0.08 L/min, and 0.1 L/min respectively. The temperature and humidity variations of the treated air at each stage under different spray flow rates are shown in Figs. 20 and 21.

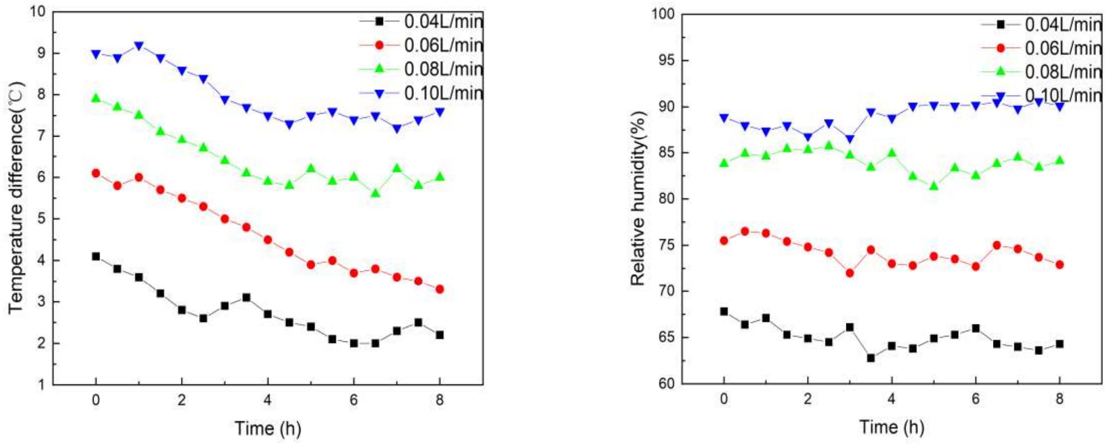

(a)Temperature difference between spray and inlet **(b) Relative humidity after spraying**

Fig. 20. The change of temperature and humidity after spraying

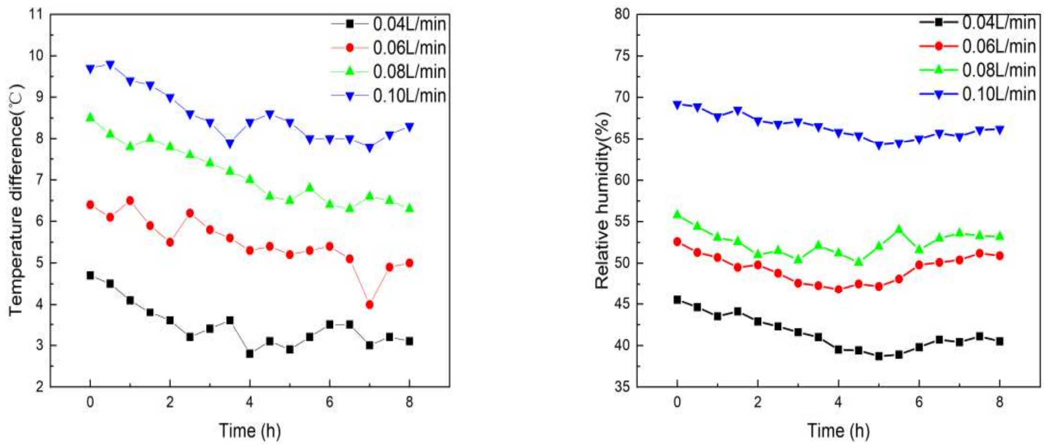

(a) Temperature difference between outlet and inlet **(b) Outlet relative humidity**

Fig. 21. The change of temperature and humidity at the outlet

Fig. 20(a) and Fig. 21(a) show that when the spray flow rate is 0.04 L/min, the temperature can be reduced by a maximum of 4.1 °C and a minimum of 2 °C through the spray section. The inlet and outlet temperatures can be reduced by a maximum of 4.7 °C and a minimum of 2.8 °C. In the PCP section, a maximum temperature reduction of 1.5 °C and a minimum of 0.5 °C can be achieved. When the spray flow rate is 0.1 L/min, the temperature reduction after passing through the spray section is a maximum of 9.2 ℃ and a minimum of 7.2 ℃. After passing through the PCP, the temperature reduction between the inlet and outlet is a maximum of 9.7 ℃ and a minimum of 7.8 ℃, with the PCP alone achieving a temperature drop of 1.3 ℃ at most and 0.3 ℃ at least. This occurs because, as the spray flow increases, the number of liquid droplets in direct contact with the air in the DEC section increases, enhancing the heat exchange volume and thus decreasing the air temperature. However, as the cooled air passes through the PCP, the temperature difference between the air and the PCM decreases, weakening the cooling effect of the PCP. From Fig. 20(b) and Fig. 21(b), it is evident that as the spray flow rate increases, the relative humidity of the air also gradually rises. However, at the same spray flow rate, the air humidity remains relatively stable. Comparatively, it can be observed that the PCP section is able to reduce the humidity by about 35 %.

4. Discussion

4.1 Analysis of the combined effect of Mult-factors

After processing and analyzing the experimental data in Section 3.2, it is concluded that outdoor fresh air can meet the air supply conditions for DCs after undergoing processing with evaporative cooling coupled with PCES technology under natural air cooling. However, the comprehensive influence of the four factors, namely, inlet temperature, inlet speed, inlet humidity, and spray flow on the integrated cooling technology remained unclear. Therefore, this study employed orthogonal experiments to analyze the combined impact of these factors on the refrigeration performance of evaporative cooling coupled with PCES technology under natural air cooling [42]. The L_{16} （4^4） form was used to conduct the orthogonal test of four factors and four levels, and the inlet temperature is 28 °C, 30 °C, 32 °C, 34 °C; inlet speed is 1 m/s, 1.5 m/s, 2 m/s, 2.5 m/s; inlet humidity is 30 %, 35 %, 40 %,45 %; spray flow is 0.04 L/min, 0.06 L/min, 0.08 L/min, 0.1 L/min, respectively. The inlet and outlet air temperature difference and outlet air relative humidity were used as indicators to quantify the cooling capability of the integrated cooling systems. Among them, a larger temperature difference indicates better cooling performance. Throughout the experiment, the outlet air relative humidity consistently met the DC air supply requirements, remaining below 80 %, which is considered satisfactory.

Table 4. Orthogonal experimental design and statistical table of experimental results

	Elements				Outlet Temperature ℃	Inlet and outlet temperature difference ℃	Outlet humidity %
	Inlet speed m/s	temperature ℃	Humidity%	Spray flow L/min			
1	1	28	30	0.04	22.8	5.2	40.5
2	1	30	35	0.06	23.1	6.9	52.2
3	1	32	40	0.08	22.5	9.5	53.8
4	1	34	45	0.1	23.9	10.1	64.3
5	1.5	28	35	0.1	23.1	4.9	66.4
6	1.5	30	40	0.04	24.1	5.9	43.7
7	1.5	32	45	0.06	24.9	7.1	45.8
8	1.5	34	30	0.08	25.2	8.8	49.6
9	2	28	40	0.08	24.5	3.5	68.8
10	2	30	45	0.1	24.2	5.8	70.4
11	2	32	30	0.04	26.1	5.9	64.9
12	2	34	35	0.06	25.9	8.1	65.7
13	2.5	28	45	0.06	25.4	2.6	70.6
14	2.5	30	30	0.08	23.4	6.6	74.1
15	2.5	32	35	0.1	25.6	6.4	77.3
16	2.5	34	40	0.04	27.2	6.8	68.3

The experimental results of the multi-factor evaporative cooling coupled PCES technology under natural air cooling were analyzed using the extreme difference method. The results are shown in Table 5. From these results, the primary and secondary factors affecting the temperature difference between the inlet and outlet of the integrated cooling system are, in order of significance: inlet temperature, inlet speed, spray flow, and inlet humidity. Furthermore, as air speed increases, the temperature difference between the inlet and outlet air decreases. At a speed of 1 m/s, the maximum temperature difference is 8.75 ℃, which is consistent with the single-factor experiments influenced by inlet speed. As the inlet temperature increases, the temperature difference between the inlet and outlet air gradually increases, reaching a maximum difference of 8.45 ℃ at an inlet temperature of 34 ℃. The impact of inlet humidity on the temperature difference is relatively minor compared to other factors, showing the smallest fluctuation range. With increasing spray flow, the temperature difference between the inlet and outlet air also shows an increasing trend. For the relative humidity of the outlet air, it is found that the relative humidity of the outlet is below 80 % under various factors, meeting the requirements for DC air supply. Based on the range analysis presented in the Table, the optimal scheme for the evaporative cooling coupled PCES technology under natural air cooling, considering multiple factors, are as follows: an inlet air speed of 1 m/s, an inlet temperature of 34 °C, an inlet humidity of 30 %, and a spray flow of 0.1 L/min.

Table 5. Range analysis

Analytical factor	Inlet and outlet air temperature difference				Relative humidity of outlet air			
level	A speed	B temperature	C humidity	D flow	A speed	B temperature	C humidity	D flow
K1	35	16.2	26.5	23.8	210.8	246.3	229.1	217.4
K2	25.4	25.2	26.3	24.7	205.5	240.4	261.6	234.3
K3	24.1	28.9	25.7	28.6	269.8	241.8	234.6	246.3
K4	22.6	33.8	25.6	30.3	290.3	247.9	251.1	278.4
k1 $(=\frac{K1}{4})$	8.75	4.05	6.625	5.95	52.7	61.575	57.275	54.35
k2 $(=\frac{K2}{4})$	6.35	6.3	6.525	6.175	51.375	60.1	65.4	58.575
k3 $(=\frac{K3}{4})$	6.025	7.225	6.425	7.15	67.45	60.45	58.65	61.575
k4 $(=\frac{K4}{4})$	5.65	8.45	6.4	7.575	72.575	61.975	62.775	69.6
range	3.1	4.4	0.225	1.625	21.2	1.875	8.125	15.25
Primary and secondary factors	B > A > D > C				A > D > C > B			

4.2 Analysis of cooling effect of temperature control system in data room

Based on the analysis in sections 3.2 and 4.1, the optimal design parameters for four influencing factors, namely inlet temperature, inlet speed, inlet humidity, and spray flow are determined to be 34 °C, 1.0 m/s, 0.1 L/min and 30 %, respectively. When the inlet temperature is reduced, the temperature difference between the air and either the water or the PCM decreases, resulting in reduced heat transfer during the corresponding stage and poor cooling performance of the integrated cooling system. As an inlet speed of 2.5 m/s, the airflow in the PCP is too fast, causing a brief contact time with the PCP and insufficient heat exchange, which compromises the humidity control capability of the cooling system. As the inlet humidity increases, the saturation of water vapor in the air gradually increases, leading to instability in the sensible heat change of the air. This results in insufficient heat and humidity exchange with water in the evaporative cooling section, reducing the cooling effect. When the spray flow is 0.04 L/min, the droplets generated by the spray are reduced in direct contact with the air, and the parts that can exchange heat and humidity with the air are also reduced.

4.3 Analysis of Innovation Points

Currently, various technologies such as air-cooling, water-cooling, and DEC have been proposed as alternatives to traditional air conditioning for DC cooling. Their advantages and disadvantages are compared in Table 6.

Considering the advantages and disadvantages of these existing technologies, we have proposed the evaporative cooling coupled with PCES technology. Utilizing a natural cooling source, this method can reduce air temperature by approximately 7 °C on average. Additionally, due to the collision between the air and the shell of the PCP, along with the partial evaporation of water vapor resulting from the temperature difference, the relative humidity of the air can be reduced by approximately 35 % in the PCP section. Consequently, the air supplied to the server room meets the ASHRAE standards for DC air supply. This approach addresses the issue of high relative humidity associated with DEC, while enabling efficient and sustained cooling for the server room, which is crucial for the development of green DCs.

Table 6. Comparative analysis

Cooling methods	Advantages	Disadvantage
natural air cooling[12, 43]	1.Clean, no pollution 2．Low cost, simple, reliable and easy to maintain	Restricted by geographical outdoor meteorological circumstances
DEC[25, 44]	1.High heat exchange efficiency 2.energy savings and low pollutant emissions	Direct vent cooling suffers from high humidity
PCES[45, 46]	1.High energy density, large latent heat 2.Low energy consumption, pollution-free 3.Long service life	Limited research on long-term cooling
Mechanical refrigeration[47-49]	1.Precise temperature control 2.high stability	high energy consumption
Evaporative cooling coupled PCES technology	1.Low electrical energy usage, no pollution 2.Not geographically restricted 3.Long-term cooling 4.Good cooling effect and moderate humidity 5.Long service life	Possible wind resistance problems with natural ventilation

4.4 Research deficiencies and suggestions

Several factors influence the evaporative cooling coupled with PCES device proposed in this study. However, due to experimental constraints, this study mainly focuses on four key factors: inlet temperature, inlet speed, inlet humidity, and spray flow, with each factor investigated through four sets of experiments. During the experiment on spray flow variation, it was observed that at a maximum inlet speed of 2.5 m/s, the relative humidity at the outlet approached 80 %, posing a safety concern. Future experimental designs may consider controlling the spray running time to balance its operation with that of the PCP, ensuring safe outlet relative humidity levels while also reducing energy consumption. For reference, Elahi et al. [50] proposed a method to control the running time of the water pump in response to the problem of low cooling capacity and efficiency using evaporative coolers at high humidity. Their findings indicated performance comparable to a two-stage indirect/direct evaporative cooler. Furthermore, future research could explore methods for water recovery or recycling from the evaporative cooling section, enhancing sustainability and efficiency in operation.

5. Concludes

To reduce energy consumption in DC cooling systems and harness renewable energy effectively, this study proposes a cooling device that integrates evaporative cooling with PCES technology under natural air cooling. The effects of inlet air temperature, inlet speed, inlet humidity, and spray flow rate on the cooling performance of the device were studied. The melting and temperature changes of the materials in the PCP were analyzed, and the changes of temperature and humidity of the air after passing through different stages of the cooling device under different working conditions were discussed. The orthogonal experiments were conducted to identify the primary and secondary factors influencing the refrigeration efficiency of the integrated cooling system. The main conclusions drawn from the study are as follows：

(1) Through experiments and analysis, the integrated cooling unit can reduce the air temperature by 10 °C-3 °C in 8 hours.

(2) For the humidity control capacity, the air humidity treated by the integrated cooling system meets the ASHRAE air supply requirements of the DC under various working conditions.

(3) For the cooling effect, the temperature difference between inlet and outlet increases with the

increase of inlet air temperature and spray flow, decreases with the increase of inlet air speed and inlet air humidity.

(4) Evaporative cooling dominates the cooling performance of the integrated cooling system, and the PCP can reduce the humidity by about 35% in addition to the cooling effect.

(5) Through orthogonal experiments, it is concluded that the primary and secondary factors affecting the cooling performance of this integrated cooling system are inlet air temperature>inlet air speed>spray flow>inlet air humidity.

(6) Through the experimental research, the outdoor fresh air in high temperature areas and other regions can be directly processed by evaporative cooling coupled PCES technology to meet the requirements of DCs air supply under extreme high temperature climate.

Declaration of competing interest

The authors declare that they have no known competing financial interests or personal relationships that could have appeared to influence the work reported in this paper.

Acknowledgments

The authors would like to thank the financial support from the National Natural Science Foundation of China (NO. 52168013 and NO.51908080), the Natural Science Foundation of Guizhou Province (No. ZK [2022]151 and No. [2020]2004), the State Key Laboratory of Gas Disaster Detecting, Preventing and Emergency Controlling Open fund Project (No.2021SKLKF10), and the College Student Innovation and Entrepreneurship Training Program Project (GZUCX2023116).

References

[1] N. Rteil, R. Bashroush, R. Kenny, A. Wynne, Interact: IT infrastructure energy and cost analyzer tool for data centers, Sustainable Computing: Informatics and Systems, 33 (2022).http://doi.org/10.1016/j.suscom.2021.100618.

[2] A. Aili, W. Long, Z. Cao, Y. Wen, Radiative free cooling for energy and water saving in data centers, Applied Energy, 359 (2024).http://doi.org/10.1016/j.apenergy.2024.122672.

[3] M. Salahuddin, K. Alam, Information and Communication Technology, electricity consumption and economic growth in OECD countries: A panel data analysis, International Journal of Electrical Power & Energy Systems, 76 (2016) 185-193.http://doi.org/10.1016/j.ijepes.2015.11.005.

[4] D. Mytton, M. Ashtine, Sources of data center energy estimates: A comprehensive review, Joule, 6(9) (2022) 2032-2056.http://doi.org/10.1016/j.joule.2022.07.011.

[5] R. Obringer, B. Rachunok, D. Maia-Silva, M. Arbabzadeh, R. Nateghi, K. Madani, The overlooked environmental footprint of increasing Internet use, Resources, Conservation and Recycling, 167 (2021).http://doi.org/10.1016/j.resconrec.2020.105389.
[6] H. Rong, H. Zhang, S. Xiao, C. Li, C. Hu, Optimizing energy consumption for data centers, Renewable and Sustainable Energy Reviews, 58 (2016) 674-691.http://doi.org/10.1016/j.rser.2015.12.283.
[7] K. Ebrahimi, G.F. Jones, A.S. Fleischer, A review of data center cooling technology, operating conditions and the corresponding low-grade waste heat recovery opportunities, Renewable and Sustainable Energy Reviews, 31 (2014) 622-638.http://doi.org/10.1016/j.rser.2013.12.007.
[8] A. Habibi Khalaj, T. Scherer, S. K. Halgamuge, Energy, environmental and economical saving potential of data centers with various economizers across Australia, Applied Energy, 183 (2016) 1528-1549.http://doi.org/10.1016/j.apenergy.2016.09.053.
[9] G. Cao, S. Zhang, Q. Zhang, G. Liu, X. Zhang, K. Yan, D. Chai, Experimental and numerical investigations of heat transfer characteristics of vertical falling film heat exchanger in data center cabinets, International Communications in Heat and Mass Transfer, 144 (2023).http://doi.org/10.1016/j.icheatmasstransfer.2023.106742.
[10] H. Endo, H. Kodama, H. Fukuda, T. Sugimoto, T. Horie, M. Kondo, Effect of climatic conditions on energy consumption in direct fresh-air container data centers, Sustainable Computing: Informatics and Systems, 6 (2015) 17-25.http://doi.org/10.1016/j.suscom.2014.03.003.
[11] X. Chen, T. Ding, L. Wang, Z. Li, Experimental research and energy effectiveness analysis on chip-level two-stage loop thermosyphon system for data centre free cooling, Applied Thermal Engineering, 245 (2024).http://doi.org/10.1016/j.applthermaleng.2024.122767.
[12] J. Zhang, R. Mao, C. Li, J. Lan, X. Yi, Z.J.A.T.E. Zhang, Optimization Air-Conditioning System and Thermal Management of Data Center via Fan-Wall Free Cooling Technology, (2023).http://doi.org/https://doi.org/10.1016/j.applthermaleng.2023.121245.
[13] U. Sajjad, N. Abbas, K. Hamid, S. Abbas, I. Hussain, S.M. Ammar, M. Sultan, H.M. Ali, M. Hussain, R. Tauseef ur, C.C. Wang, A review of recent advances in indirect evaporative cooling technology, International Communications in Heat and Mass Transfer, 122 (2021).http://doi.org/10.1016/j.icheatmasstransfer.2021.105140.
[14] Y. Jing, L. Xie, F. Li, Z. Zhan, Z. Wang, F. Yang, J. Fan, Z. Zhu, H. Zhang, C. Zhao, Z. Shi, H. Jiang, X. Xie, Y. Jiang, Field test of cooling systems in two air-cooled data centers: Various regions, air distributions and evaporative cooling technologies, Applied Thermal Engineering, 248 (2024).http://doi.org/10.1016/j.applthermaleng.2024.123189.
[15] X. Cui, C. Yang, W. Yan, X. Wang, Y. Liu, L. Jin, Climatic applicability of indirect evaporative cooling strategies for data centers in China, Journal of Building Engineering, 83 (2024).http://doi.org/10.1016/j.jobe.2023.108431.
[16] G. Lv, X. Ji, B. Yang, Y. Chen, H.J.A.T.E. Xu, Operating modes study of evaporative cooling-dehumidification air conditioning under different climatic conditions, (2024).http://doi.org/https://doi.org/10.1016/j.applthermaleng.2024.122597.
[17] M. Hnayno, A. Chehade, H. Klaba, G. Polidori, C. Maalouf, Experimental investigation of an optimized indirect free cooling system including a dry cooler equipped with evaporative cooling pads for data center, Energy Reports, 9 (2023) 460-469.http://doi.org/10.1016/j.egyr.2023.12.005.

[18] A.A.R. Darzi, S.M. Moosania, F.L. Tan, M. Farhadi, Numerical investigation of free-cooling system using plate type PCM storage, International Communications in Heat and Mass Transfer, 48 (2013) 155-163.http://doi.org/10.1016/j.icheatmasstransfer.2013.08.025.
[19] M. Rogowski, R.J.I.C.i.H. Andrzejczyk, M. Transfer, Recent advances of selected passive heat transfer intensification methods for phase change material-based latent heat energy storage units: A review, (2023).http://doi.org/https://doi.org/10.1016/j.icheatmasstransfer.2023.106795.
[20] J.-X. Wang, J. Qian, N. Wang, H. Zhang, X. Cao, F. Liu, G. Hao, A scalable micro-encapsulated phase change material and liquid metal integrated composite for sustainable data center cooling, Renewable Energy, 213 (2023) 75-85.http://doi.org/10.1016/j.renene.2023.05.106.
[21] B. Huang, Z. Zheng, G. Lu, X. Zhai, Design and experimental investigation of a PCM based cooling storage unit for emergency cooling in data center, Energy and Buildings, 259 (2022).http://doi.org/10.1016/j.enbuild.2022.111871.
[22] J. Yuan, Y. Yan, X. Zhang, X. Kong, T.J.A.T.E. Zhang, Coupling of flexible phase change materials and servers for improving the security of data centers in emergency situations, (2024).http://doi.org/https://doi.org/10.1016/j.applthermaleng.2024.122439.
[23] V. Ljungdahl, M. Jradi, C.J.A.T.E. Veje, A decision support model for waste heat recovery systems design in data center and high-performance computing clusters utilizing liquid cooling and phase change materials, (2021).http://doi.org/https://doi.org/10.1016/j.applthermaleng.2021.117671.
[24] M. Gholampour, Z.-W. Zhang, C.-C. Wang, Extending air-cooled data center emergency cooling duration with phase change material: An experimental study, Journal of Building Engineering, 90 (2024).http://doi.org/10.1016/j.jobe.2024.109439.
[25] C. Li, R. Mao, Y. Wang, J. Zhang, J. Lan, Z. Zhang, Experimental study on direct evaporative cooling for free cooling of data centers, Energy, 288 (2024).http://doi.org/10.1016/j.energy.2023.129889.
[26] P. Liu, R. Kandasamy, J.Y. Ho, T.N. Wong, K.C.J.E. Toh, Dynamic performance analysis and thermal modelling of a novel two-phase spray cooled rack system for data center cooling, (2023).http://doi.org/https://doi.org/10.1016/j.energy.2023.126835.
[27] W. Liu, S. Cheng, J. Wang, H. Wang, Z. Liu, Z. Geng, S. Zhang, S. He, J. Qi, K. Han, M. Gao, Y.J.A.T.E. Shi, Numerical study on the cooling performance of various arrangements of medium-gap-medium for direct evaporative cooling systems, (2024).http://doi.org/https://doi.org/10.1016/j.applthermaleng.2023.121921.
[28] J. Shim, S. Ki, D. Seo, B. Moon, S. Bang, Y. Nam, Intermittent spray cooling on rationally-designed hierarchical surfaces for enhanced evaporative heat transfer performance, International Communications in Heat and Mass Transfer, 153 (2024).http://doi.org/10.1016/j.icheatmasstransfer.2024.107354.
[29] A. Waqas, S.J.T.L. Kumar, Thermal performance of latent heat storage for free cooling of buildings in a dry and hot climate: A, (2011).http://doi.org/https://doi.org/10.1016/j.enbuild.2011.06.015.
[30] J. Zamani, A.J.I.C.i.H. Keshavarz, M. Transfer, Genetic algorithm optimization for double pipe heat exchanger PCM storage system during charging and discharging processes, (2023).http://doi.org/https://doi.org/10.1016/j.icheatmasstransfer.2023.106904.

[31] R.V. Seeniraj, N.L.J.I.C.i.H. Narasimhan, M. Transfer, The thermal response of a cold LHTS unit with heat leak through side walls, 32 (2005) 1375-1386.http://doi.org/https://doi.org/10.1016/j.icheatmasstransfer.2005.07.011.
[32] J. Sun, K. Nawaz, J. Rendall, A. Elatar, J.J.I.C.i.H. Brechtl, M. Transfer, Heat pump water heater enhanced with phase change materials thermal energy storage: Modeling study, (2023).http://doi.org/https://doi.org/10.1016/j.icheatmasstransfer.2023.106917.
[33] B.E. Kareem, A.M. Adham, B.N.J.J.o.B.E. Yaqob, Experimental analysis of air-multiple pcm heat exchanger in evaporative cooling systems for supply air temperature stabilization, (2024).http://doi.org/https://doi.org/10.1016/j.jobe.2023.108269.
[34] V.A.A. Raj, R.J.R. Velraj, S.E. Reviews, Review on free cooling of buildings using phase change materials, 14 (2010) 2819-2829.http://doi.org/https://doi.org/10.1016/j.rser.2010.07.004.
[35] P. B, V.A. A, G. P, A.M.M.S. A, A.J.R. T, S.E. Reviews, Solar photovoltaic cooling using Paraffin phase change material: Comprehensive assessment, (2024).http://doi.org/https://doi.org/10.1016/j.rser.2024.114372.
[36] A. Sharma, V.V. Tyagi, C.R. Chen, D. Buddhi, Review on thermal energy storage with phase change materials and applications, Renewable and Sustainable Energy Reviews, 13(2) (2009) 318-345.http://doi.org/10.1016/j.rser.2007.10.005.
[37] E. Hasrati, A.J.I.C.i.H. Jain, M. Transfer, Dual-sided melting of a one-dimensional composite wall comprising two distinct phase change material (PCM) layers, (2024).http://doi.org/https://doi.org/10.1016/j.icheatmasstransfer.2023.107207.
[38] R.J.J.o.H.T.-t.o.T.A. Viskanta, Heat Transfer During Melting and Solidification of Metals, 110 (1988) 1205-1219.http://doi.org/https://doi.org/10.1115/1.3250621.
[39] S. Shao, H. Liu, H. Zhang, C.J.E. Tian, Experimental investigation on a loop thermosyphon with evaporative condenser for free cooling of data centers, (2019).http://doi.org/https://doi.org/10.1016/j.energy.2019.07.095.
[40] J.C. Cortés, L. Jódar, L.J.J.C.A.M. Villafuerte, Mean square solution of Bessel differential equation with uncertainties, 309 (2017) 383-395.http://doi.org/https://doi.org/10.1016/j.cam.2016.01.034.
[41] E.J.J.C.A.M. Denich, Error estimates for a Gaussian rule involving Bessel functions, 436 (2023) 115448.http://doi.org/https://doi.org/10.1016/j.cam.2023.115448.
[42] M. Chen, Z. Zhang, Q. Deng, Y. Feng, X. Wang, Optimization of underfloor air distribution systems for data centers based on orthogonal test method: A case study, Building and Environment, 232 (2023).http://doi.org/10.1016/j.buildenv.2023.110071.
[43] L. Wu, R. Mao, H. Wu, J. Zhang, C. Li, X. Yi, G. Huang, Z.J.A.T.E. Zhang, Optimization of airflow organization in fan-wall data center via baffles, (2024).http://doi.org/https://doi.org/10.1016/j.applthermaleng.2024.122745.
[44] Y.-C. Lee, K.-Y. Chen, W.-M. Yan, Y.-C. Shih, C.-Y. Chao, Evaporative cooling method to improve energy management of overhead downward flow-type data center, Case Studies in Thermal Engineering, 45 (2023).http://doi.org/10.1016/j.csite.2023.102998.
[45] Y. Xiang, G.J.E. Zhou, Buildings, Thermal performance of a window-based cooling unit using phase change materials combined with night ventilation, 108 (2015) 267-278.http://doi.org/https://doi.org/10.1016/j.enbuild.2015.09.030.
[46] M.J. Hosseini, A.A. Ranjbar, K. Sedighi, M.J.I.C.i.H. Rahimi, M. Transfer, A combined experimental and computational study on the melting behavior of a medium temperature phase

change storage material inside shell and tube heat exchanger, 39 (2012) 1416-1424.http://doi.org/https://doi.org/10.1016/j.icheatmasstransfer.2012.07.028.
[47] K. Ebrahimi, G.F. Jones, A.S.J.R. Fleischer, S.E. Reviews, A review of data center cooling technology, operating conditions and the corresponding low-grade waste heat recovery opportunities, 31 (2014) 622-638.http://doi.org/https://doi.org/10.1016/j.rser.2013.12.007.
[48] G.I. Meijer, Cooling Energy-Hungry Data Centers, 328(5976) (2010) 318-319.http://doi.org/doi:10.1126/science.1182769.
[49] M. Santamouris, D.J.E. Kolokotsa, Buildings, Passive cooling dissipation techniques for buildings and other structures: The state of the art, 57 (2013) 74-94.http://doi.org/https://doi.org/10.1016/j.enbuild.2012.11.002.
[50] S.H. Elahi, S.J.I.C.i.H. Farhani, M. Transfer, Increasing evaporative cooler efficiency by controlling water pump run and off times, 127 (2021) 105525.http://doi.org/https://doi.org/10.1016/j.icheatmasstransfer.2021.105525.